

# Compartmentalization of Incompatible Reagents within Pickering Emulsion Droplets for One-Pot Cascade Reactions

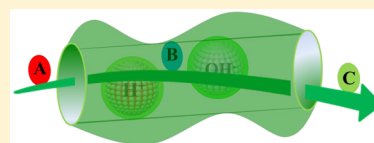
Hengquan Yang,<sup>\*,†</sup> Luman Fu,<sup>†</sup> Lijuan Wei,<sup>†</sup> Jifen Liang,<sup>†</sup> and Bernard P. Binks<sup>‡</sup>

<sup>†</sup>School of Chemistry and Chemical Engineering, Shanxi University, Wucheng Road 92, Taiyuan 030006, China

<sup>‡</sup>Surfactant and Colloid Group, Department of Chemistry, University of Hull, Hull HU6 7RX, U.K.

**S** Supporting Information

**ABSTRACT:** It is a dream that future synthetic chemistry can mimic living systems to process multistep cascade reactions in a one-pot fashion. One of the key challenges is the mutual destruction of incompatible or opposing reagents, for example, acid and base, oxidants and reductants. A conceptually novel strategy is developed here to address this challenge. This strategy is based on a layered Pickering emulsion system, which is obtained through lamination of Pickering emulsions. In this working Pickering emulsion, the dispersed phase can separately compartmentalize the incompatible reagents to avoid their mutual destruction, while the continuous phase allows other reagent molecules to diffuse freely to access the compartmentalized reagents for chemical reactions. The compartmentalization effects and molecular transport ability of the Pickering emulsion were investigated. The deacetalization–reduction, deacetalization–Knoevenagel, deacetalization–Henry and diazotization–iodization cascade reactions demonstrate well the versatility and flexibility of our strategy in processing the one-pot cascade reactions involving mutually destructive reagents.



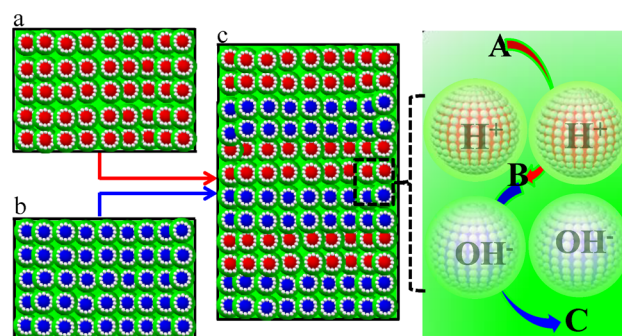
## 1. INTRODUCTION

Living systems can process multistep cascade chemical transformations to produce complex molecules.<sup>1</sup> One key concept living systems adopt is “compartmentalization”, through which incompatible or opposing reagents are spatially isolated to avoid mutual destruction.<sup>2–5</sup> This concept is, however, still a dream for non-natural systems.<sup>6–9</sup> Recently, many non-natural systems have been suggested,<sup>10,11</sup> which mainly rely on immobilization or encapsulation of incompatible reagents with sol–gel materials,<sup>12–20</sup> or polymers,<sup>21–31</sup> avoiding their direct contact. Although these attempts lead to encouraging results, these methods are applied only in particular cases and are not very versatile because they either require relatively complex immobilization/encapsulation procedures or need special polymers. Moreover, these cascade systems are still embryonic because of the inability to mimic the fundamental aspects of natural systems.

Particle-stabilized emulsions [called Pickering emulsions, oil-in-water (o/w) or water-in-oil (w/o)] might make the dream come true,<sup>32–38</sup> because the whole system is divided into numerous separate droplets that can serve as microcompartments and even protocells.<sup>39–42</sup> Moreover, in Pickering emulsions, the oil and water phases are sufficiently mixed leading to a high area of oil–water interface available for chemical reactions.<sup>43–48</sup> It has recently been found that such a micromixing enables organic–aqueous biphasic reactions to proceed efficiently through the autodiffusion of reactant molecules (without the need for stirring), and the reaction efficiency is as high as that achieved with vigorous stirring.<sup>49</sup> We envision that these unique properties of a Pickering emulsion could be helpful to address the obstacles of biomimetic synthesis if its architecture was innovatively constructed so as to

effectively compartmentalize incompatible reagents but allow other reactants to diffuse freely in reaction systems. However, Pickering emulsion-based cascade reactions have not been explored up to date.

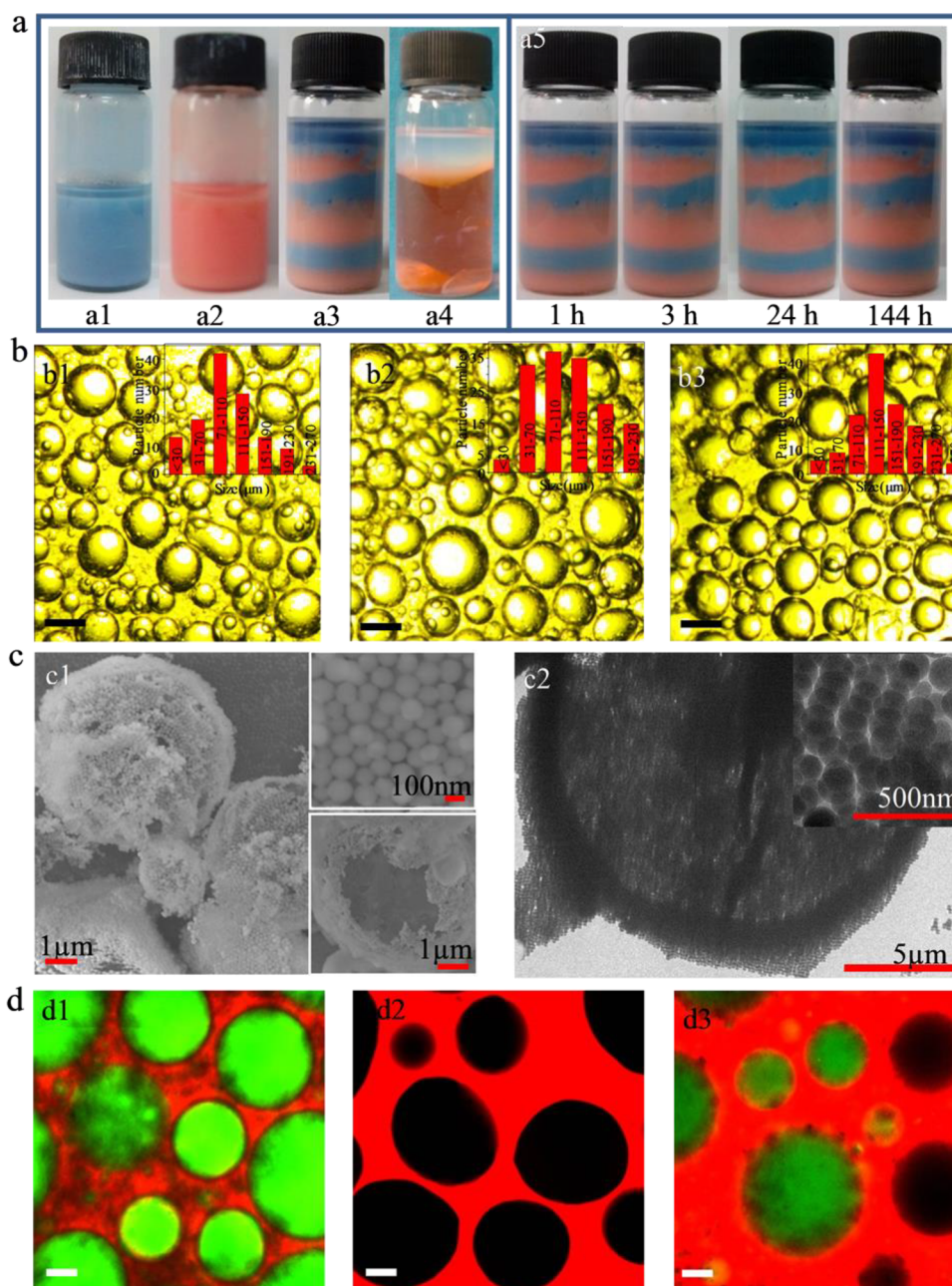
Herein, we demonstrate a conceptually novel strategy to perform one-pot cascade reactions involving opposing reagents based on Pickering emulsions. As Figure 1 shows, one can first



**Figure 1.** Schematic description of a one-pot cascade reaction based on the proposed Pickering emulsion strategy ( $A \rightarrow B \rightarrow C$ , where  $A$  is the starting substrate,  $B$  represents the intermediate and  $C$  is the final product). (a) The w/o Pickering emulsion was formulated with water-soluble acid, water, starting substrate  $A$  and oil phase. (b) The w/o Pickering emulsion was formulated with water-soluble base, water and oil phase. (c) Mixing a and b through a lamination procedure leads to a layered Pickering emulsion system, which serves as a medium for one-pot cascade reactions.

Received: December 3, 2014

Published: December 30, 2014



**Figure 2.** Appearance of the layered Pickering emulsions in the presence of indicator and the microstructures of emulsion droplets. (a) Appearance of the Pickering emulsions in the presence of Congo Red: (a1) The Pickering emulsion was formulated with 4 mL of HCl (0.01 M), 1.8 mL of toluene, 0.3 g of methyl-modified SiO<sub>2</sub> and 0.001 g of Congo Red; (a2) The Pickering emulsion was formulated with 4 mL of NaOH (0.01 M), 1.8 mL of toluene, 0.3 g of methyl-modified SiO<sub>2</sub> and 0.001 g of Congo Red; (a3) The Pickering emulsion was obtained by mixing a and b through lamination; (a4) The mixture was obtained by mixing two mixtures that were the same as a and b in composition but not emulsified; (a5) The layered Pickering emulsion after standing for 1, 3, 24, and 144 h. (b) Optical microscopy images (b1–b3, scale bar is 200  $\mu\text{m}$ ): (b1) Image of a, a1; (b2) Image of a, a2; (b3) Image of a, a3. (c) SEM and TEM images of emulsion droplets: (c1) SEM images obtained after freezing-drying (the upper inset reflects the packing of silica nanoparticles and the lower inset reflects the hollow structure of microcompartments); (c2) TEM images obtained at low temperature. (d) Fluorescent confocal microscopy images of the Pickering emulsion droplets (d1–d3, scale bar is 100  $\mu\text{m}$ ) before and after mixing: (d1) Dispersed phase of Pickering emulsion was stained with FITC-dextran and its continuous phase was stained with Nile red; (d2) Dispersed phase was not stained and its continuous phase was stained with Nile red; (d3) Mixed Pickering emulsion after standing for 4 h.

prepare two parent water-in-oil Pickering emulsions using nanoparticles as emulsifier. In one Pickering emulsion, a reagent, e.g., acid as catalyst or reactant, is dissolved in the water droplets (dispersed phase) and a reactant A is dissolved in the oil phase (continuous phase, Figure 1a). In the other Pickering emulsion, a reagent, e.g., base as catalyst or reactant, is also dissolved in the water droplets (Figure 1b) and other

reactants are dissolved in the continuous phase if needed. These two parent Pickering emulsions with opposing reagents are then brought into contact through lamination (Figure 1c), yielding a multilayered Pickering emulsion system for cascade reactions. The layered architecture allows the positioning of the emulsion droplets in different regions to avoid direct contact. During the course of reaction, the acid and base are

compartmentalized in the water droplets and should not get in contact with each other avoiding destruction. Meanwhile, the reactant A in the continuous (oil) phase can freely move through autodiffusion, and is converted to the intermediate B upon meeting the acid at the droplet interface, which is subsequently transformed to the final product C after meeting the base-contained droplets located in the neighboring layer. In this scenario, the whole Pickering emulsion reaction system is just like a living system, which can spatially position diverse cells in different regions, compartmentalize the mutually destructive enzymes or molecules in the different cells but allow for the free diffusion of other molecules located outside the cells for biochemical reactions if needed.

## 2. RESULTS AND DISCUSSION

### 2.1. Compartmentalization Effects of Water Droplets.

Although surfactant-stabilized emulsions were reported to have the ability to compartmentalize opposing reagents, the trapping time is only several minutes, which is too short to carry out chemical reactions.<sup>50</sup> The dynamic exchanges of molecular surfactant between emulsion droplets and the presence of free surfactant in the continuous phase probably accelerate mass transport of the molecules between different droplets.<sup>51,52</sup> Moreover, after the completion of reaction, the separation of surfactants from products is relatively difficult. These obstacles may be overcome with particle-stabilized emulsions. Partially hydrophobic silica nanospheres with diameters of 130–200 nm were used as emulsifier, which were easily prepared from bare silica particles through a one-step modification with methyltrimethoxysilane [transmission electron microscopy (TEM) images, scanning electron microscopy (SEM) images and particle size distribution are included in Figure S1 (Supporting Information)]; the methyl group loading is estimated to be 0.072 mmol g<sup>-1</sup> (ca. 3 methyl groups per square nm) on the basis of elemental analysis; the thermogravimetric curves are displayed in Figure S2; the air–water contact angle of the particle surfaces is 91°, as shown in Figure S3].

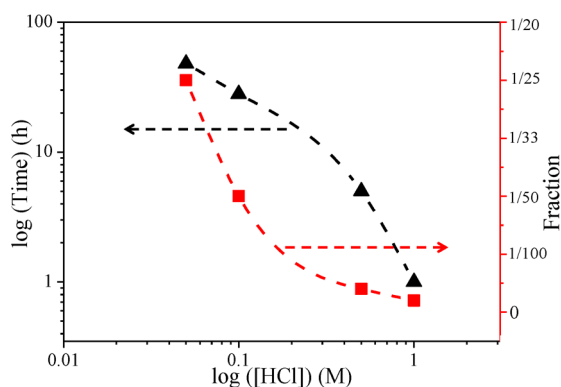
We first checked the feasibility of the coexistence of opposing reagents, e.g., HCl and NaOH, in a single vessel with the proposed Pickering emulsion strategy. Congo Red was used as indicator to visualize the pH changes of water droplets because it is exclusively water-soluble (not oil-soluble) and its color varies in response to pH changes (azure at pH < 3.0 and red at pH > 5.0). Two parent water-in-toluene Pickering emulsions were formulated with acidic or basic solutions of Congo Red (the water volume fraction of each Pickering emulsion is ca. 70%). The use of a solution of HCl (0.01 M) led to an azure-colored Pickering emulsion (Figure 2, a1), while the use of a solution of NaOH (0.01 M) resulted in a red-colored Pickering emulsion (Figure 2, a2). Mixing these two Pickering emulsions through a lamination procedure yielded a new Pickering emulsion, which exhibited zebra stripes with alternate azure and red colors (Figure 2, a3). The layered architecture was successfully achieved since no agitation is implemented during the course of mixing. However, in a control experiment, mixing two mixtures that were the same as a1 and a2 Pickering emulsions in composition (including toluene, water, particle emulsifier, acid or base, and indicator) but not emulsified, led to a suspension that rapidly changed to red color (Figure 2, a4), which is a result of acid–base reactions. These comparisons underline that Pickering emulsions are crucial to obtain an acid/base-coexisting system. More importantly, after standing for 1, 3, and 24 h, the appearance of layered Pickering

emulsions remained virtually the same, and there was still a clear boundary between the layers without color fading (Figure 2, a5). Impressively, after this layered Pickering emulsion stood for 144 h, the zebra stripes of alternate colors were still well maintained indicating the survival of acid and base in the same system. Such a period of time is sufficiently long for most chemical reactions themselves to take place. In contrast, the surfactant-stabilized emulsions have poor ability to achieve the survival of acid and base in a single system (Figure S4).

In order to investigate these results further, optical microscopy, SEM and TEM were employed to observe the microstructures of the Pickering emulsions. Before mixing, the Pickering emulsions formulated with HCl and NaOH consist of droplets with diameters ranging from around 10 to 250 μm (Figure 2, b1 and b2). After mixing via a lamination procedure and further standing for 24 h, the morphology and size distribution of the emulsion droplets sampled from close to a layer boundary show no apparent changes (Figure 2, b3). This indicates that the layered Pickering emulsions have high stability against droplet coalescence and Ostwald ripening, and thereby have excellent ability to create stable microcompartments. The microcompartments created by emulsion droplets were further confirmed by SEM. After the layered Pickering emulsion (close to a layer boundary) was treated by freeze-drying, microspheres were clearly observed (Figure 2, c1), which originated from precursor emulsion droplets. In the more magnified SEM image (Figure 2, upper inset of c1), silica nanospheres are observed to be closely packed on the surface of these microspheres. As expected, the microspheres are hollow (Figure 2, lower inset of c1) since freeze-drying involves removal of the inner water directly from a solid to a gas. This is direct evidence for the pronounced microcompartments. Similar to the SEM image, the TEM image obtained at low temperature further confirmed the droplet microstructure (Figure 2, c2). The excellent ability to prevent acid–base neutralizations can be attributed to the microcompartments within Pickering emulsions.

To further confirm the compartmentalization effects of droplets, we used fluorescence microscopy to observe whether reagent molecules transfer between droplets. Two parent Pickering emulsions were formulated in the presence of fluorescent dyes (there is no acid or base in the water in these experiments). The first was prepared with water containing FITC-dextran (green) and toluene containing Nile red (red). Judging by the colors of Figure 2, d1 (green inside droplets and red outside droplets), this Pickering emulsion is of the water-in-oil type since FITC-dextran is a water-soluble dye while Nile red is an oil-soluble one. The second was prepared with pure water (without FITC-dextran) and toluene containing Nile red. As seen in Figure 2, d2, the continuous phase is red while the interior of the droplets is black because of the absence of fluorescent dye molecules. These two Pickering emulsions were also put in contact via a lamination procedure. After standing for 4 h, the emulsion droplets close to a layer boundary were withdrawn and observed with fluorescence microscopy. Notably, green droplets and black ones were both observed (Figure 2, d3). That is to say, the FITC-dextran dye molecules did not enter the initially dye-free droplets over this time scale. These findings further confirm that the formulated Pickering emulsion has a good ability to compartmentalize molecules within water droplets and to prevent the transfer of these molecules to other droplets despite the large concentration gradient.

To quantify the effectiveness of the layered architecture in preventing the neutralization of acid and base, we conducted a set of more sensitive experiments in which one Pickering emulsion containing a high concentration of HCl was laminated onto the other Pickering emulsion containing a low concentration of NaOH and Congo Red indicator. In such experiments, if only a small portion of HCl diffuse out from water droplets and cross the oil film to react with NaOH at the layer boundary, the color of the layer boundary should change. The concentration of HCl was increased from 0.05 to 0.1, 0.5, and 1 M while the concentration of NaOH was always kept constant (0.001 M). After these two-layered Pickering emulsions stood for a period of time, the color of a layer boundary was observed to change from the initial red to the somewhat azure color (Figure S5). Interestingly, the larger the concentration of HCl, the shorter the time taken for this color change to occur. As shown in Figure 3, when the HCl



**Figure 3.** Time for layer boundary to change color and the fraction of the neutralized acid for the four layered Pickering emulsion systems. The layered Pickering emulsions were obtained by lamination of one Pickering emulsion containing a high concentration of HCl onto another Pickering emulsion containing a low concentration of NaOH and Congo Red indicator. [HCl] was changed from 0.05 to 1 M while [NaOH] was kept constant at 0.001 M.

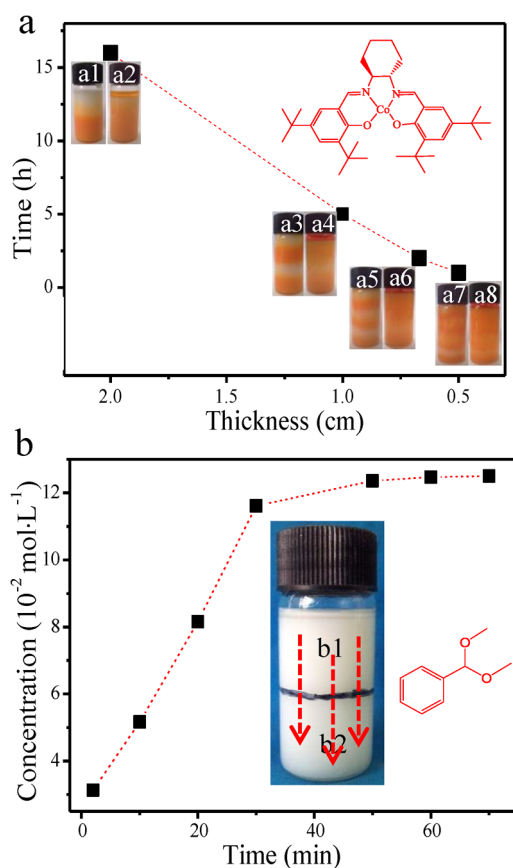
concentration increases from 0.05 to 0.1, 0.5, and 1 M, the time taken for the color change at the layer boundary falls from 48 to 28, 5, and 1 h, respectively. This can be explained by the high concentration gradient accelerating HCl diffusion. Based on the indicator color change, one can estimate that only ca. 1/25, 1/50, 1/250 and 1/500 of the initial HCl at the layer boundary of the layered Pickering emulsion reacted with NaOH. Notably, for these Pickering emulsions, the lower red layer and the upper white layer remained unchanged even after standing for at least 35 h, indicating that the neutralized acid and base in the overall Pickering emulsion system is at a negligible level. This set of sensitive experiments sufficiently confirms the high effectiveness of our layered Pickering emulsion strategy.

Our further investigations show that the excellent stability to compartmentalize opposing reagents in water droplets is mainly contributed by three factors: (i) The first is the layered architecture. For the Pickering emulsion system obtained by lamination followed by gentle mixing (3 min, homogeneously mixing the droplets), the coexistence of acid and base in a single vessel was found to be maintained for only 3 h, and after this period the initial azure Pickering emulsion gradually became red as shown in Figure S6. The comparison with the results achieved with the above layered Pickering emulsion without stirring confirms that the layered architecture is more

effective to prevent the destruction of opposing reagents in a single system. The reason may be that the layered architecture significantly decreases the possibility of direct contact of droplets containing opposing reagents. (ii) The second is the concentration of solid particle emulsifier. It was found that a high concentration of solid particle emulsifier is favorable to prevent the mutual destruction of the opposing reagents. As Figure S7 shows, when the concentration of particles was decreased from 7.5 to 0.375 wt % (with respect to water), HCl and NaOH can only survive in a single vessel up to 3 h. (iii) The third is the solubility of compartmentalized reagents. As shown in Figure S8, when NaOH was changed to other bases such as  $\text{NH}_2\text{CH}_2\text{CH}_2\text{NH}_2$  and  $\text{HOCH}_2\text{CH}_2\text{NH}_2$  that are only soluble in water (not oil-soluble), their coexistence with acid-containing droplets without reaction was up to at least 144 h. In contrast, for  $\text{NH}(\text{CH}_2\text{CH}_3)_2$  that is both water-soluble and oil-soluble, the acid–base reaction is complete within 3 h. This implies that the solubility of the reagents in the continuous phase plays a key role, and only opposing reagents that are not soluble in the continuous phase can be effectively compartmentalized without destruction. A reasonable explanation is that the continuous phase constitutes an oil film that separates droplets, and the low solubility of compartmentalized reagents in the oil film can significantly impede their mass transport.

**2.2. Molecule Transport in the Continuous Phase.** We next check the molecular transport ability of the continuous phase of layered Pickering emulsions. The coordination complex *N,N'*-bis(3,5-di-*tert*-butylsalicylidene)ethylenediamino-cobalt(II) [Co(Salen)] was chosen as a probe molecule since it is oil-soluble and its red color is helpful to observe molecular transport. A layered Pickering emulsion was obtained by mixing one Pickering emulsion in the presence of Co(Salen) with an equal volume of the other Pickering emulsion in the absence of Co(Salen) (without acid and base in this experiment). By varying the total layer numbers from 2 to 4, 6 and 8, the thickness of each layer was adjusted from 2.0 to 1.0, 0.67, and 0.50 cm, as shown in Figure 4a (a1, a3, a5 and a7, respectively). Initially, these Pickering emulsions were observed to consist of zebra stripes with alternate red and white colors. After standing for a period of time, the white layer became red suggesting that Co(Salen) molecules diffuse throughout the whole volume of the vessel (Figure 4a, a2, a4, a6 and a8; the color changes are displayed in detail in Figure S9). It was found that the thinner the layer, the quicker this takes place. For the Pickering emulsions with layer thickness of 0.5 cm (a7 and a8), it took only 40 min to complete homogeneous distribution, which is relatively short in comparison with the time scale for most chemical reactions. These observations confirm that the continuous phase of a layered Pickering emulsion system allows the transport of molecules through autodiffusion.

The good transport ability of the layered Pickering emulsions is further demonstrated with an alternative probe molecule benzaldehyde dimethylacetal (only oil-soluble). For ease of monitoring, a two-layered Pickering emulsion was formulated with benzaldehyde dimethylacetal initially in the upper layer (Figure 4b). Gas chromatography (GC) was used to determine the concentration of benzaldehyde dimethylacetal at the bottom of the vessel. It was found that the concentration of benzaldehyde dimethylacetal at the bottom gradually increased with time and leveled off after ca. 40 min, suggesting that benzaldehyde dimethylacetal was homogeneously distributed throughout the vial through molecular diffusion. In comparison with the experiment with Co(Salen) (two-layered Pickering



**Figure 4.** Molecular transport in the continuous phase of layered Pickering emulsions. (a) The time taken by Co(Salen) to diffuse throughout the whole volume of the vessel as a function of the layer thickness. The insets are photos of the initial state (left) and state of reaching homogeneous distribution (right). The structure of Co(Salen) is also given. The detailed procedure is included in Supporting Information, Materials. (b) Concentration of benzaldehyde dimethylacetal at the bottom of vial as a function of time. The detailed procedure for this experiment is included in Supporting Information. b1 represents the upper layer of Pickering emulsion where benzaldehyde dimethylacetal is initially dissolved; b2 is the lower layer of Pickering emulsion where benzaldehyde dimethylacetal is initially absent.

emulsion), the time is much shorter, which may be explained in terms of different diffusion coefficients.

We use Fick's second law to estimate the time taken for organic reactants to reach homogeneous distribution between layers, which is given by the equation

$$\frac{\partial C}{\partial t} = D \frac{\partial^2 C}{\partial x^2} \quad (1)$$

where  $C$  is the concentration of diffusing species,  $t$  the time,  $D$  the diffusion coefficient of the diffusing species and  $x$  is the distance diffused. Assuming that no reaction occurs and the presence of droplets is ignored, the solution<sup>53</sup> to the equation with initial boundary conditions  $C_0(x, 0) = C_0$  in even layers and  $C(x, 0) = 0$  in odd layers is

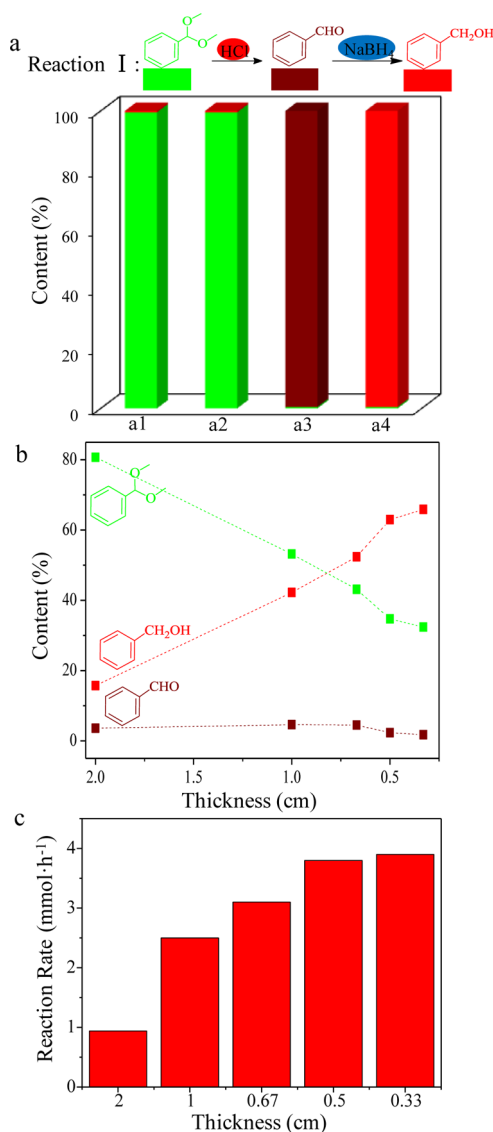
$$C(x, t) = \frac{1}{2}C_0 + \sum_{n=0}^{\infty} \frac{(-1)^n}{(2n+1)\pi} \exp\left\{-\frac{\pi^2(2n+1)^2Dt}{4L^2}\right\} \cos\left\{\frac{\pi(2n+1)x}{2L}\right\} \quad (2)$$

where the sum is over all values of  $n$  from 0 to  $\infty$ , and  $L$  is the half layer thickness. This is an infinite series with terms getting smaller as  $n$  increases.

$$C(x, t) = \frac{1}{2}C_0 + \frac{2C_0}{\pi} \exp\left\{-\frac{\pi^2Dt}{4L^2}\right\} \cos\left\{\frac{\pi x}{2L}\right\} - \frac{2C_0}{3\pi} \exp\left\{-\frac{9\pi^2Dt}{4L^2}\right\} \cos\left\{\frac{3\pi x}{2L}\right\} + \frac{2C_0}{5\pi} \exp\left\{-\frac{25\pi^2Dt}{4L^2}\right\} \cos\left\{\frac{5\pi x}{2L}\right\} - \frac{2C_0}{7\pi} \exp\left\{-\frac{49\pi^2Dt}{4L^2}\right\} + \dots \quad (3)$$

The eq 3 has many exponentials with decay times  $\tau$ ,  $\tau/9$ ,  $\tau/25$ ,  $\tau/49$ , ..., where  $\tau = (4L^2)/(\pi^2D)$ . In this case,  $\tau$  is the longest time scale. It can be estimated that the time for a reactant to reach homogeneous distribution between layers is 0.07–7 h for a layer thickness of 0.5 cm and a diffusion coefficient  $D$  in the range of  $1 \times 10^{-8}$ – $10^{-10}$  m<sup>2</sup> s<sup>-1</sup>. Such a time scale is acceptable for most reactions since the diffusion time scale and reaction time scale are the same order of magnitude. Moreover, we believe for a given reaction, this time may be significantly shortened because the local concentration gradients caused by chemical reactions can accelerate the molecular diffusion since the molecular diffusion rate scales with the square of the concentration gradient.

**2.3. One-Pot Cascade Reactions.** Given the above encouraging results, we next examined this Pickering emulsion strategy with one-pot cascade reactions. A deacetalization–reduction cascade reaction was first chosen, in which deacetalization was catalyzed with HCl and reduction required NaBH<sub>4</sub> (Reaction I in Figure 5). HCl and NaBH<sub>4</sub> is a pair of opposing reagents because they rapidly react with each other. Normally, it is impossible to combine these two reactions in a single vessel. To validate the examination, we conducted a set of control experiments and all reactions were carried out without stirring at room temperature. The reaction systems were formulated by mixing two mixtures. In the first control experiment, one mixture consisted of an aqueous solution of HCl, toluene, silica particle emulsifier, and benzaldehyde dimethylacetal, while the other comprised an aqueous solution of NaBH<sub>4</sub>, toluene and silica particle emulsifier. Despite the presence of particle emulsifier, these two mixtures were not emulsified before mixing, thereby consisting of toluene and water layers. It was observed that bubbles were rapidly produced upon mixing, caused by the reaction of HCl with NaBH<sub>4</sub> releasing H<sub>2</sub>. After standing for 30 min, the content of benzaldehyde dimethylacetal in the reaction mixture was determined to be more than 99% (first bar of Figure 5a) and the content of the final product benzyl alcohol was less than 0.5%. In the second control experiment, these two mixtures were first emulsified (stirring for 2 min) and were then mixed through a lamination procedure (0.33 cm in layer thickness, 3 + 3 layers), but in the first Pickering emulsion HCl is absent.



**Figure 5.** Results of one-pot deacetalization–reduction cascade reaction. (a) Final compositions of the deacetalization–reduction reactions in different systems. Green represents benzaldehyde dimethylacetal; brown represents benzaldehyde and red represents benzyl alcohol. Composition of the reaction system: 0.5 mmol benzaldehyde dimethylacetal, 4 mL of water, 1.8 mL of toluene, 0.02 mmol HCl (if used), 1.5 mmol NaBH<sub>4</sub> (if used), and 0.3 g of methyl-modified SiO<sub>2</sub>. Reaction conditions: 25 °C and 30 min. (a1) The reaction system in the presence of both HCl and NaBH<sub>4</sub> but without emulsification; (a2) The Pickering emulsion system in the absence of HCl; (a3) The Pickering emulsion system in the absence of NaBH<sub>4</sub>; (a4) The Pickering emulsion system in the presence of both HCl and NaBH<sub>4</sub>. (b) The reaction results versus the layer thickness (the reaction scale is the double of that described in a and the total volume is 11.6 mL). The contents of benzaldehyde dimethylacetal, benzaldehyde and benzyl alcohol were determined by GC when the reaction proceeded for 10 min. Their total contents are 100%. (c) The reaction rate (moles of benzyl alcohol generated per h) versus the layer thickness (the reaction scale is the double of that described in a and the total volume is 11.6 mL).

After the same time, the content of benzaldehyde dimethylacetal in the reaction mixture was also more than 99% (second bar of Figure 5a) and the reaction did not occur. In the third control experiment, these two mixtures were emulsified and were then mixed through the same procedure as the second

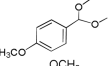
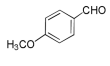
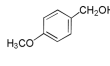
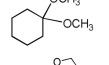
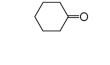
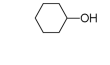
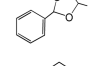
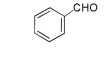
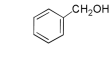
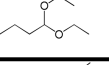
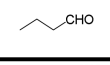
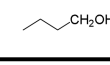
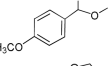
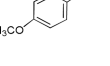
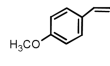
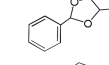
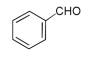
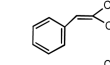
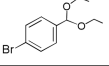
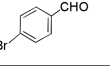
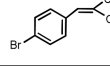
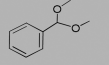
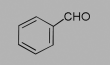

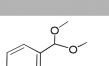
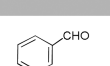

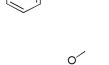
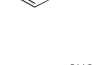

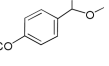
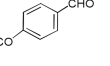
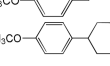
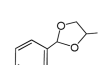
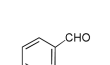
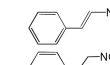
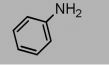
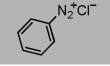
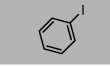
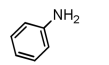
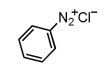
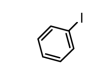
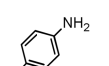
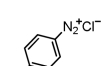
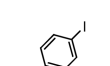
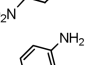
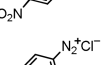
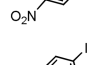
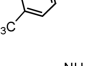
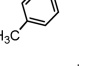
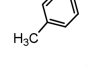
control experiment, but in the second Pickering emulsion NaBH<sub>4</sub> was not introduced. After 30 min, benzaldehyde dimethylacetal was completely converted to the intermediate benzaldehyde, but the final product benzyl alcohol was not detected (third bar of Figure 5a). These control experiments suggest that both the emulsification and combination of HCl and NaBH<sub>4</sub> are absolutely necessary for this cascade reaction. We then checked this one-pot cascade reaction in the presence of both HCl and NaBH<sub>4</sub> with our layered Pickering emulsion strategy (0.33 cm in layer thickness, 3 + 3 layers). After the same period of time, benzaldehyde dimethylacetal was fully transformed to the final product benzyl alcohol via a deacetalization–reduction cascade (final bar of Figure 5a). These comparisons confirm the effectiveness of our Pickering emulsion strategy in one-pot cascade reactions involving opposing catalyst and reactant.

To clarify the impact of the layer thickness on the reaction systems we varied the layer number from 2 to 4, 6, and 8. The thickness of each layer was correspondingly changed from 2.0 to 1.0, 0.67, 0.50, and 0.33 cm. After a period of 10 min, the contents of benzaldehyde dimethylacetal, benzylaldehyde and benzyl alcohol in each Pickering emulsion system were determined. The layer thickness-dependent contents for the reactant, intermediate and product are reflected in Figure 5b. As the layer thickness decreases, the content of benzaldehyde dimethylacetal decreases from 80 to 53, 43, 35 and 32%, the content of benzyl alcohol increases from 16 to 42, 52, 63 and 66%. Notably, in each Pickering emulsion system, the content of the intermediate benzaldehyde was always lower than 5% and the accumulation of the intermediate did not occur during the whole course of reaction. This means that once the deacetalization reaction starts the reduction reaction occurs and these two reactions proceed simultaneously, which is a feature of one-pot cascade reactions.

On the basis of the content of the generated final product benzyl alcohol, one can estimate the reaction rate of the Pickering emulsion systems, defined as the moles of the final product per hour. As displayed in Figure 5c, the reaction rate of the layered Pickering emulsion system is closely related to the layer thickness of the reaction systems, and it increases upon decreasing the layer thickness. However, when the layer thickness is decreased beyond to 0.50 cm, the reaction rate no longer increases significantly. Such a dependence can be interpreted with the aforementioned molecular diffusion equation. The shorter the diffusion distance, the shorter the time for the reactant to complete the homogeneous distribution. When the layer thickness decreases to a certain level for a given reaction, the reaction rate is no longer suppressed by the reactant diffusion rate. These findings suggest that the reaction rate of one-pot cascade systems can be regulated through changing the layer thickness.

The deacetalization–reduction cascade reaction (Reaction I) can be applied to other substrates, as summarized in Table 1. All examined reactions were formulated with a layer thickness of 0.33 cm (3 + 3 layers) and carried out without stirring. Methoxybenzaldehyde dimethylacetal was completely converted to the final product methoxybenzyl alcohol within 0.5 h at room temperature, and the intermediate methoxybenzaldehyde was not detected. Cyclohexanone dimethylacetal was also fully transformed to the final product cyclohexanol within 2 h. For the less reactive acetals such as benzaldehyde propylene glycolacetal and butaldehyde diethylacetal, the content of the final products were determined as 99% within

Table 1. Results of Four One-Pot Cascade Reactions with Different Pairs of Opposing Reagents<sup>a</sup>

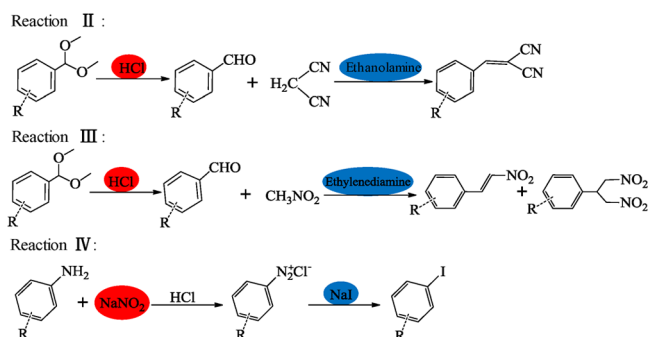
Cascade reactions	Reactants	Intermediates	Products	T/°C	t/h <sup>b</sup>	B/% <sup>c</sup>	C/% <sup>d</sup>
I				25	0.5	0	>99
				25	2	0	>99
				50	2	1	99
				50	2	1	99
II				25	10	5	84
				60	10	13	75
				60	10	13	78
III				70	10	0	0.3 <sup>e</sup> 0.3 <sup>c</sup>
				70	10	12	40 40
				70	18	28	28 38
				70	18	16	58 22
				70	18	16	58 22
IV				25	24	/	0.8 <sup>e</sup>
				25	2.5	/	91
				25	0.3	/	93
				25	5	/	86
				25	4	/	72

<sup>a</sup>Reaction I is shown in Figure 5 and its reaction conditions are similar to the statements in Figure 5; Reactions II, III and IV are displayed in Figure 6; The reaction conditions are described in Supporting Information. <sup>b</sup>Reaction time. <sup>c,d</sup>The yields of the intermediate B and the final product C except Reaction I; For Reaction I, the data are the contents of the intermediate B and the final product C in the final mixture. <sup>e</sup>Control experiments without preparing a Pickering emulsion.

2 h at 50 °C. These findings demonstrate the versatility and effectiveness of the Pickering emulsion strategy.

The versatility and effectiveness of the Pickering emulsion strategy is further demonstrated by other cascade reactions involving different pairs of opposing reagents. Figure 6 displays another three cascade reactions in which opposing reagents are marked with different colors: deacetalization–Knoevenagel condensation cascade (Reaction II, acid/base pair); deacetalization–Henry cascade (Reaction III, acid/base pair), and diazotization–iodization cascade (Reaction IV, oxidant/reductant pair). The results of these three cascade reactions are also

summarized in Table 1. For Reaction II, in the absence of emulsion droplets or HCl or ethanolamine, it is impossible to get the final product in a satisfactory yield (Figure S10). However, with the Pickering emulsion strategy, all the investigated acetals were found to undergo a complete deacetalization and the isolated yields of final dicyano compounds were between 75 and 84% within 10 h. For Reaction III, the control experiment also shows that without emulsification very little product was detected. In contrast, with the Pickering emulsion strategy the final products including



**Figure 6.** Extended one-pot cascade reactions in the presence of a pair of opposing reagents. Reaction II: the deacetalization–Knoevenagel cascade reaction in the presence of HCl/ethanolamine pair; Reaction III: the deacetalization–Henry cascade in the presence of HCl/ethylenediamine pair; Reaction IV: the diazotization–iodization cascade in the presence of  $\text{NaNO}_2/\text{NaI}$  pair.

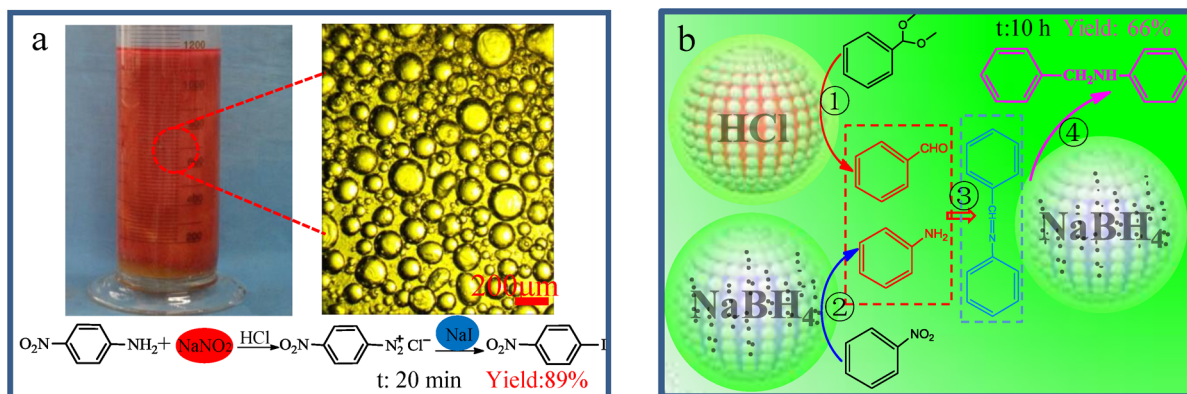
$\alpha,\beta$ -unsaturated nitro and dinitro compounds were obtained. Their total yields were up to 66–80% within 10–18 h.

Reaction IV was explored here to synthesize aryl iodides in one-pot. The conventional process of synthesizing aryl iodide consists of two separate reactions: diazotization and iodination. Only after the diazotization is complete can NaI be added for the second reaction because NaI is otherwise quickly oxidized by  $\text{NaNO}_2$  under the reaction conditions. Moreover, there is a serious risk of explosion due to the accumulation of unstable diazonium in the reaction system.<sup>54</sup> With the Pickering emulsion strategy (0.33 cm in layer thickness, 3 + 3 layers),  $\text{NaNO}_2$  and NaI were compartmentalized in the different droplets. As shown in Table 1 for the investigated reactants, the iodide yields are as high as 72–93% in a one-pot reaction. In our multiple experiments, explosion was not observed. As Figure S11 exhibits, the concentration of diazonium intermediate was always kept below  $5 \times 10^{-5}$  M during the course of reaction. The accumulation of unstable diazonium in the reaction system does not occur in our cascade systems. The intermediate diazonium formed is transformed instantaneously into iodides, which significantly decreases the risk of explosion.

**2.4. Scaling up One-Pot Cascade Reactions.** In order to examine the practical application feasibility of our Pickering emulsion strategy, the scale of the diazotization–iodization cascade (Reaction IV) was increased up to 1 L (Figure 7a). The

scaled-up reaction system was easily obtained through mixing two Pickering emulsions with a lamination procedure (0.6 cm of the layer thickness), similar to the milliliter-scaled reaction. After standing for 20 min, the conversion of 4-amino nitrobenzene was complete. About 20 g of 4-iodo nitrobenzene was obtained and the isolated yield was as high as 89%. The reaction efficiency does not significantly decrease after scaling-up in terms of reaction time and yield. This may be ascribed to the fact that the Pickering emulsion phase and emulsion droplet sizes were well maintained despite scale-up (Figure 7a) creating large reaction interface areas. Notably, during the reaction process,  $\text{N}_2$  bubbles were observed to be released progressively, as diazonium is smoothly transformed into iodide. Moreover, the silica nanoparticles were easily separated from products through a filtrate step for reuse. In the second batch, the isolated yield of 4-iodo nitrobenzene was still up to 85% within the same reaction time.

**2.5. One-Pot Multiple Cascade Reactions.** The versatility of our Pickering emulsion strategy is further highlighted by a one-pot four cascade reaction for synthesizing mono *N*-alkyl amine in the presence of solid catalysts. Using nitrobenzene and benzaldehyde dimethylacetal as starting materials, the whole synthesis process comprises four separate reactions: (1) reduction of nitrobenzene to aniline with  $\text{NaBH}_4$  in the presence of a Pd catalyst, (2) deacetalization of benzaldehyde dimethylacetal to benzaldehyde in the presence of HCl, (3) condensation of aniline with benzaldehyde to yield imine, and (4) reduction of imine with  $\text{NaBH}_4$  to the final product mono *N*-alkyl amine. Normally, the four reaction cascade is impossible to realize because of the destruction of  $\text{NaBH}_4$  and HCl. As shown in Figure 7b (and Figure S12), the cascade reaction system was obtained by mixing two Pickering emulsions. In one, methyl-modified silica blended with a small amount of an interfacially active catalyst  $\text{Pd}/\text{SiO}_2\text{-CN}(4)$  was used as emulsifier,<sup>45</sup> where  $\text{Pd}/\text{SiO}_2\text{-CN}(4)$  also acted as catalyst for the nitrobenzene and imine reduction. After standing for 10 h at 60 °C, the starting materials benzaldehyde dimethylacetal and nitrobenzene were not detected, and the final product *N*-alkyl amine was obtained in a yield of 66% (the yield of main side product benzyl alcohol was 21%). The high reaction efficiency is attributed to the formation of a Pickering emulsion, which enables multiple reagents including water-soluble reagents, oil-soluble ones and solid catalysts to be



**Figure 7.** Scaling-up of a one-pot cascade reaction and a one-pot four-step cascade reaction in the presence of solid catalyst. (a) The diazotization–iodization cascade scaled up to 1 L, for which the reaction conditions are included in Supporting Information. The photo of the vessel was taken at the end of reaction. (b) The one-pot four step cascade reaction for synthesizing *N*-alkyl aniline, of which the reaction conditions are included in the Supporting Information.



sufficiently mixed. These results further demonstrate that our Pickering emulsion strategy is highly flexible to allow multicomponent, multistep cascade reactions even in the presence of solid catalysts.

### 3. CONCLUSIONS

We have demonstrated a novel strategy for one-pot cascade reactions based on the lamination of Pickering emulsions. The droplets of this working Pickering emulsion system have proven able to separately compartmentalize incompatible or opposing reagents to avoid mutual destruction, while its continuous phase allows other reagent molecules to diffuse freely to access the compartmentalized reagents for chemical reactions. Such compartmentalization and efficient mass transport under static conditions constitute the fundamental features of biomimetic multistep synthesis to some extent, which are difficult to obtain with the existing methods. As a proof of the concept, the deacetalization–reduction, deacetalization–Knoevenagel, deacetalization–Henry and diazotization–iodization cascade reactions demonstrate well the applicability, versatility and flexibility of our strategy in processing one-pot cascade reactions involving incompatible reagents. Being simple, versatile and efficient, our strategy provides an unprecedented opportunity to practical cascade reactions with mutually destructive reagents.

### ■ ASSOCIATED CONTENT

#### Supporting Information

Experimental details; TEM and SEM images; TG curves; water contact angles; appearance of various Pickering emulsions; results of the deacetalization–Knoevenagel cascade reaction in different systems; results of monitoring diazonium concentration; optical microscopy image; NMR and MS data for products. This material is available free of charge via the Internet at <http://pubs.acs.org>.

### ■ AUTHOR INFORMATION

#### Corresponding Author

hgyang@sxu.edu.cn

#### Notes

The authors declare no competing financial interest.

### ■ ACKNOWLEDGMENTS

The authors thank Dr. R. Ettelaie, University of Leeds, for his help with the theoretical estimations. This work was financially supported by the Natural Science Foundation of China (20903064, 21173137), Program for New Century Excellent Talents in University (NECT-12-1030), Program for the Top Young Academic Leaders of Higher Learning Institutions of Shanxi (2011002) and Middle-aged Innovative Talents of Higher Learning Institutions of Shanxi (20120202).

### ■ REFERENCES

- (1) Agapakis, C. M.; Boyle, P. M.; Silver, P. A. *Nat. Chem. Biol.* **2012**, *8*, 527.
- (2) Longstreet, A. R.; McQuade, D. T. *Acc. Chem. Res.* **2013**, *46*, 327.
- (3) Fischlechner, M.; Schaerli, Y.; Mohamed, M. F.; Patil, S.; Abell, C.; Hollfelder, F. *Nat. Chem.* **2014**, *6*, 791.
- (4) Marguet, M.; Bonduelle, C.; Lecommandoux, S. *Chem. Soc. Rev.* **2013**, *42*, 512.
- (5) Weitz, M.; Mückl, A.; Kapsner, K.; Berg, R.; Meyer, A.; Simmel, F. C. *J. Am. Chem. Soc.* **2014**, *136*, 72.

- (6) Wasilke, J. C.; Obrey, S. J.; Baker, R. T.; Bazan, G. C. *Chem. Rev.* **2005**, *105*, 1001.
- (7) Nightingale, A. M.; Phillips, T. W.; Bannock, J. H.; de Mello, J. C. *Nat. Commun.* **2014**, *5*, 3777.
- (8) Yamada, Y.; Tsung, C. K.; Huang, W. Y.; Huo, Z. Y.; Habas, S. E.; Soejima, T.; Aliaga, C. E.; Somorjai, G. A.; Yang, P. D. *Nat. Chem.* **2011**, *3*, 372.
- (9) Grondal, C.; Jeanty, M.; Enders, D. *Nat. Chem.* **2010**, *2*, 167.
- (10) Voit, B. *Angew. Chem., Int. Ed.* **2006**, *45*, 4238.
- (11) Filice, M.; Palomo, J. M. *ACS Catal.* **2014**, *4*, 1588.
- (12) Gelman, F.; Blum, J.; Avnir, D. *J. Am. Chem. Soc.* **2000**, *122*, 11999.
- (13) Gelman, F.; Blum, J.; Avnir, D. *Angew. Chem., Int. Ed.* **2001**, *40*, 3647.
- (14) Shi, J. F.; Wang, X. L.; Zhang, W. Y.; Jiang, Z. Y.; Liang, Y. P.; Zhu, Y. Y.; Zhang, C. H. *Adv. Funct. Mater.* **2013**, *23*, 1450.
- (15) Marr, A. C.; Marr, P. C. *Dalton Trans.* **2011**, *40*, 20.
- (16) Gelman, F.; Blum, J.; Avnir, D. *J. Am. Chem. Soc.* **2002**, *124*, 14460.
- (17) Motokura, K.; Fujita, N.; Mori, K.; Mizugaki, T.; Ebitani, K.; Kaneda, K. *J. Am. Chem. Soc.* **2005**, *127*, 9674.
- (18) Yang, Y.; Liu, X.; Li, X. B.; Zhao, J.; Bai, S. Y.; Liu, J.; Yang, Q. H. *Angew. Chem., Int. Ed.* **2012**, *51*, 9164.
- (19) Climent, M. J.; Corma, A.; Iborra, S. *ChemSusChem* **2009**, *2*, 500.
- (20) Pilling, A. Q.; Beohmer, J.; Dixon, D. J. *Angew. Chem., Int. Ed.* **2007**, *46*, 5428.
- (21) Helms, B.; Guillaudeu, S. J.; Xie, Y.; McMurdo, M.; Hawker, C. J.; Fréchet, J. M. J. *Angew. Chem., Int. Ed.* **2005**, *44*, 6384.
- (22) Brett Runge, M.; Mwangi, M. T.; Lee Miller, A., II; Perring, M.; Bowden, N. B. *Angew. Chem., Int. Ed.* **2008**, *47*, 935.
- (23) Wang, Z. P.; van Oers, M. C. M.; Rutjes, F. P. J. T.; van Hest, J. C. M. *Angew. Chem., Int. Ed.* **2012**, *51*, 10746.
- (24) Shi, J. F.; Wang, X. L.; Zhang, W. Y.; Jiang, Z. Y. *ACS Appl. Mater. Interfaces* **2011**, *3*, 881.
- (25) Kékicheff, P.; Schneider, G. F.; Decher, G. *Langmuir* **2013**, *29*, 10713.
- (26) Peters, R. J. R. W.; Marguet, M.; Marais, S.; Fraaije, M. W.; van Hest, J. C. M.; Lecommandoux, S. *Angew. Chem., Int. Ed.* **2014**, *53*, 146.
- (27) Merino, E.; Verde-Sesto, E.; Maya, E. M.; Iglesias, M.; Sánchez, F.; Corma, A. *Chem. Mater.* **2013**, *25*, 981.
- (28) Poe, S. L.; Kobašljica, M.; McQuade, D. T. *J. Am. Chem. Soc.* **2006**, *128*, 15586.
- (29) Chi, Y. G.; Scroggins, S. T.; Fréchet, J. M. J. *J. Am. Chem. Soc.* **2008**, *130*, 6322.
- (30) Peters, R. J. R. W.; Louzao, I.; van Hest, J. C. M. *Chem. Sci.* **2012**, *3*, 335.
- (31) Chen, Z. W.; Zhou, L.; Bing, W.; Zhang, Z. J.; Li, Z. H.; Ren, J. S.; Qu, X. G. *J. Am. Chem. Soc.* **2014**, *136*, 7498.
- (32) Tu, F. Q.; Lee, D. *J. Am. Chem. Soc.* **2014**, *136*, 9999.
- (33) Tsuji, S.; Kawaguchi, H. *Langmuir* **2008**, *24*, 3300.
- (34) Yan, N. X.; Gray, M. R.; Masliyah, J. H. *Colloids Surf., A* **2001**, *193*, 97.
- (35) Read, E. S.; Fujii, S.; Amalvy, J. I.; Randall, D. P.; Armes, S. P. *Langmuir* **2004**, *20*, 7422.
- (36) Zhou, W. J.; Fang, L.; Fan, Z. Y.; Albel, B.; Bonnevot, L.; De Campo, F.; Pera-Titus, M.; Clacens, J. M. *J. Am. Chem. Soc.* **2014**, *136*, 4869.
- (37) Keating, C. D. *Nat. Chem.* **2013**, *5*, 449.
- (38) Wu, C. Z.; Bai, S.; Ansorge-Schumacher, M. B.; Wang, D. Y. *Adv. Mater.* **2011**, *23*, 5694.
- (39) Chandrawati, R.; van Koeveden, M. P.; Lomas, H.; Caruso, F. *J. Phys. Chem. Lett.* **2011**, *2*, 2639.
- (40) Li, M.; Harbron, R. L.; Weaver, J. V. M.; Binks, B. P.; Mann, S. *Nat. Chem.* **2013**, *5*, 529.
- (41) Dinsmore, A. D.; Hsu, M. F.; Nikolaidis, M. G.; Marquez, M.; Bausch, A. R.; Weitz, D. A. *Science* **2002**, *298*, 1006.

- (42) Huang, X.; Li, M.; Green, D. C.; Williams, D. S.; Patil, A. J.; Mann, S. *Nat. Commun.* **2013**, *4*, 2239.
- (43) Crossley, S.; Faria, J.; Shen, M.; Resasco, D. E. *Science* **2010**, *327*, 68.
- (44) Wiese, S.; Spiess, A. C.; Richtering, W. *Angew. Chem., Int. Ed.* **2013**, *52*, 576.
- (45) Yang, H. Q.; Zhou, T.; Zhang, W. J. *Angew. Chem., Int. Ed.* **2013**, *52*, 7455.
- (46) Leclercq, L.; Company, R.; Mühlbauer, A.; Mouret, A.; Aubry, J. M.; Nardello-Rataj, V. *ChemSusChem* **2013**, *6*, 1533.
- (47) Fu, L. M.; Li, S. R.; Han, Z. Y.; Liu, H. F.; Yang, H. Q. *Chem. Commun.* **2014**, *50*, 10045.
- (48) Zhu, Z. B.; Tan, H. Y.; Wang, J.; Yu, S. Z.; Zhou, K. B. *Green Chem.* **2014**, *16*, 2636.
- (49) Zhang, W. J.; Fu, L. M.; Yang, H. Q. *ChemSusChem* **2014**, *7*, 391.
- (50) Dunstan, T. S.; Fletcher, P. D. I. *Langmuir* **2011**, *27*, 3409.
- (51) Malassagne-Bulgarelli, N.; McGrath, K. M. *Soft Matter* **2009**, *5*, 4804.
- (52) Calderó, G.; García-Celma, M. J.; Solans, C.; Pons, R. *Langmuir* **2000**, *16*, 1668.
- (53) *Diffusion*, 3rd ed.; Cussler, E. L., Ed.; Cambridge University Press: Cambridge, U.K., 2009.
- (54) Mo, F. Y.; Dong, G. B.; Zhang, Y.; Wang, J. B. *Org. Biomol. Chem.* **2013**, *11*, 1582.